Nanocomposite Li-Ion Battery Anodes Produced by the Partial Reduction of Mixed Oxides

Pimpa Limthongkul, Haifeng Wang, and Yet-Ming Chiang*

Department of Materials Science and Engineering, Massachusetts Institute of Technology, Cambridge, Massachusetts 02139

Received December 29, 2000. Revised Manuscript Received April 17, 2001

A method based on the thermochemical reduction of mixed oxides is demonstrated for creating ultrafine metal−ceramic composites for lithium storage. Mixed oxides containing a more noble metal, selected to be capable of alloying with lithium at potentials useful as a Li-ion battery anode, are partially reduced to form electrochemically active composites of the dispersed metal in a conductive oxide matrix. The starting oxides $SbVO_4$ rutile and $Sb_2Mn_2O_7$ distorted fluorite are discussed as examples. Materials are characterized using XRD, SEM, and TEM, and electrochemical tests are presented. Reversible charge capacities of 300−400 mAh/g (1800−2500 mAh/cm^3) are shown to be possible in these systems.

Introduction

Increasing demand for higher energy density battery systems has motivated an ongoing search for new storage electrodes with high gravimetric and volumetric charge capacity and excellent cycleability. Carbon is presently used as the negative electrode in Li-ion rechargeable batteries due to its high capacity (372 mAh/g and 837 mAh/cm^3), good cycleability, and low cost.[1] Due to their high theoretical energy densities, a number of Li-metal alloy systems have also been investigated as candidates for negative electrodes.[2−4] However, because of the large volume changes and mechanical failure that accompanies Li cycling, capacity retention upon cycling is usually poor.

Research in tin oxide containing anodes[5,6] shows that improved cycleability is possible if the metal phase is electrochemically reduced in-situ to ultrafine particulates. These oxides especially offer higher volumetric capacity than carbon (>1800 mAh/cm^3) and can exhibit good cycleability, but a major limiting factor is the large irreversibility loss during the first cycle, due to irreversible lithium consumption accompanying the initial electrochemical reduction of tin oxide to tin metal.[6] Reduction of first cycle irreversibility while retaining good cycleability has been described[7,8] for some composites containing ultrafine dispersions of lithium-active metals produced by mechanical milling. These studies suggest that fine dispersions of lithium-active metals can be robust anodes.[3−4,8,9]

In the present research, the partial reduction of mixed oxides using simple thermochemical processes has been explored as an alternative approach to fabricating electrochemically active metal−ceramic nanocomposites with reduced first-cycle irreversibility loss and in which phase and volume changes during lithium insertion and removal can be accommodated. Experiments have been conducted in several systems, as discussed more completely elsewhere.[10] Here we focus on oxides in the Sb−V−O and Sb−Mn−O family to illustrate of this general approach.

Partial Reduction

In partial reduction reactions a ternary or higher order oxide (or nitride, sulfide, etc.) is subjected to thermochemical conditions that reduce the most noble metal(s) but leaves the less noble metal(s) in an oxidized form:[11]

$$\mathrm{Me^{I}}_a\mathrm{Me^{II}}_b\mathrm{O}_c \xrightarrow[\text{reduced}]{\text{partially}} a\mathrm{Me^{I}} + \mathrm{Me^{II}}_b\mathrm{O}_y + (c-y)/2\mathrm{O}_2 \quad (1)$$

Here Me^{I} is more noble than Me^{II}. Depending on the starting composition and the relative diffusion rates of oxygen and the cations, either internal reduction, wherein the reduced species precipitates inside an oxide matrix, or external reduction, wherein the reduced species forms at the outer surface, can occur.[11] Examples of previously studied systems include Mg−Me−O (Me = Ni, Co, Fe, Cu), Al−Me−O (Me = Cr, Fe, Ni), Fe−Mn−O, and Fe−Cr−O.[13−18] While partial reduction

(1) Megahed, S.; Scrosati, B. *J. Power Sources* **1994**, *51*, 79.
(2) Fauteux, D.; Koksbang, P. *J. Appl. Electrochem.* **1993**, *23*, 1.
(3) Huggins, R. A. *J. Power Sources* **1989**, *26*, 109.
(4) Yang, J.; Winter, M.; Besenhard, J. O. *Solid State Ionics* **1996**, *90*, 281.
(5) Idota, Y.; Kubota, T.; Matsufuji, A.; Maekawa, Y.; Miyasaka, T. *Science* **1997**, *276*, 1395.
(6) Courtney, I. A.; Dahn, J. *J. Electrochem. Soc.* **1997**, *144*, 2045.
(7) Mao, O.; Turner, R. L.; Courtney, I. A.; Fredericsen, B. D.; Buckett, M. I.; Krause, L. J.; Dahn, J. R. *Electrochem. Solid State Lett.* **1999**, *2* (1), 3.
(8) Ehrlich, G. M.; Durand, C.; Chen, X.; Hugener, T. A.; Spiess, F.; Suib, S. L. *J. Electrochem. Soc.* **2000**, *147* (3), 886.
(9) Courtney, I. A.; Dahn, J. R. *J. Electrochem. Soc.* **1997**, *144* (9), 2942.
(10) Limthongkul, P.; Wang, H.; Chiang, Y.-M. *Electrochemical Society Proceedings, Symposium on Rechargeable Lithium Batteries*; 198th Meeting of the Electrochemical Society, Phoenix, AZ, Oct 22−27, 2000; Electrochemical Society: Pennington, NJ, in press.
(11) Schmalzried H.; Backhaus-Ricoult, M. *Prog. Solid State Chem.* **1993**, *22*, 1.
(12) Narayan, J.; Chen, Y. *Philos. Mag.* **1984**, *A49*, 475.

10.1021/cm0014280 CCC: $20.00
Published on Web 06/12/2001

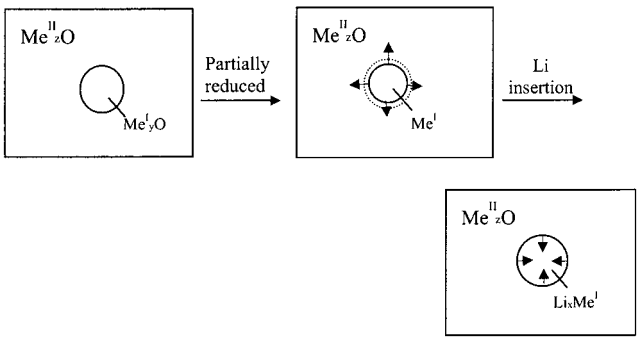

Figure 1. Schematic illustrating partial reduction of a mixed oxide producing an internal metal precipitate Me^I of reduced volume in an oxide Me^{II}_zO, followed by lithiation of the metal to an alloy Li_xMe^I with accompanying volume expansion.

reactions have been studied as a basic phenomenon[13,18] and used for fabricating materials for potential applications as structural materials[14−15,19] and optical storage media,[16,20] to our knowledge this is the first instance where it has been used to synthesize electrochemically active materials.

For use as a lithium storage electrode, our objective is to produce fine particles of a lithium-active metal, Me^I, enclosed within or dispersed among particles of a metal−oxide matrix $Me^{II}_bO_y$. The matrix itself may or may not be lithium active. Materials made by this process can have a number of advantages: (1) First-cycle irreversibility can be reduced since the electrochemically driven displacement reactions that Li_2O forms as a byproduct upon first lithium insertion[6] can be avoided. These displacement reactions are typically irreversible or poorly reversible. (2) Ultrafine metal particles, which appear to better tolerate cyclic volume changes than coarser particles or bulk metal,[4,9,21] can be produced. Partial reduction can produce metal particles as small in diameter as a few nanometers. (3) Volume shrinkage of the metal oxide upon reduction can provide room for the subsequent expansion of the metal upon lithiation (Figure 1). Note that the total volume change from starting oxide to lithiated compound can be almost zero for some systems. (4) Chemical compatibility between cell components may be improved. Passivating layers are known to exist between pure elemental negative electrodes and liquid electrolytes. Where internal reduction of a partially reduced mixed oxide is achieved, the active metal particles can be isolated from the electrolyte by an oxide that is more chemically compatible. (5) High electronic and ionic conductivity of the composite can be achieved. Transition metal oxides are among the most attractive candidates for the host metal oxide $Me^{II}_yO_z$ for this reason.

Selection Criteria for Partially Reduced Anodes

Since most metals studied to date alloy at voltages <1 V relative to lithium metal, they are primarily suitable for the anode in rechargeable lithium batteries. Criteria for choosing a starting mixed oxide $(Me^I-Me^{II})_aO_b$ include the following: (i) For high energy density, Me^I should alloy with Li at a low voltage with respect to lithium metal and high Li/Me^I ratio. Low atomic mass and high density for both Me^I and $Me^{II}_yO_z$ are preferred to obtain high gravimetric and volumetric capacity. (ii) The oxides of Me^I and Me^{II} should form an intermediate compound or solid solution. Immiscibility can be useful if fine-scale phase separation can be obtained.[10] (iii) The Gibbs free energy of oxidation for Me^I must be reasonably less negative than that of Me^{II} so as to allow latitude in processing temperature and atmosphere. That is, Me^I should lie significantly above Me^{II} on the Ellingham diagram. (iv) The net molar volume change from reduction of the starting oxide Me^IaO_b through lithiation to the compound Li_xMe^I should be as low as possible (Figure 1). (v) $Me^{II}_yO_z$ is preferably a good electronic and lithium ion conductor. (vi) Low-cost and nontoxic metals and metal oxides are preferred.

The generality of our approach is indicated by the fact that, upon searching the JCPDS database, over 100 compounds have been found that meet most or all of the above criteria. Partial reduction experiments on several mixed oxides has in each instance resulted in electrochemically active composites.[10] However, as we show, the electrochemical performance especially upon extended cycling depends also on the microstructure that is obtained. Within the general approach of partial reduction, we have identified three specific strategies for obtaining fine dispersions of the metal within an oxide matrix: (1) The concentration and relative diffusivity of the lithium-active metal can be selected to obtain internal vs external reduction, in oxides with low oxygen diffusivity;[11] (2) Systems of high oxygen diffusivity for which internal reduction is always expected can be selected. (3) Phase separation can be conducted prior to reduction in order to confine the reduced metal phase. Although each of these three approaches has been experimentally demonstrated,[10] in this paper we focus on specific Sb-bearing oxides in order to illustrate the impact of external vs internal reduction on electrochemical properties.

Model Starting Compounds: $SbVO_4$ and $Sb_2Mn_2O_7$. Sb is of interest for lithium storage since it can alloy up to 3 Li/Sb atom, giving a theoretical charge capacity of 661 Ah/kg (4415 mAh/cm^3) at a voltage plateau of 0.94−0.96 V relative to Li metal.[22] The volumetric expansion upon lithiating Sb is large, being a factor of 1.97 for forming Li_2Sb and 2.35 for forming Li_3Sb. However, note that the molar volumes of Sb_2O_5 and Li_3Sb are almost equal (42.57 and 42.74 cm^3/mol, respectively), resulting in nearly zero volume change if the oxide is reduced to Sb metal and then lithiated to

(13) Ostyn, K. M.; Carter, C. B.; Koehne, M., Falke, H.; Schmalzried, H. *J. Am. Ceram. Soc.* **1984**, *67*, 679.
(14) Subramanian, R.; Üstündag, E.; Sass, S. L.; Dieckmann, R. *Mater. Sci. Eng.* **1995**, *A195*, 51.
(15) Üstündag, E.; Subramanian, R.; Dieckmann, R.; Sass, S. L. *Acta Metall. Mater.* **1995**, *43*, 383.
(16) Smith, J. A.; Limthongkul, P.; Hartsuyker, L.; Kim, S. Y.; Sass, S. L. *J. Appl. Phys.* **1998**, *83*, 2719.
(17) Ricoult D. L.; Schmalzried, H. *J. Mater. Sci.* **1987**, *22*, 2257.
(18) Schmalzried, H. *Ber. Bunsen-Ges. Phys. Chem.* **1984**, *88*, 1186.
(19) Smith, J. A.; Limthongkul, P.; Sass, S. L. *Processing and Fabrication of Advanced Materials IV*; Srivatsan, T. S., Moore, J. J., Eds.; The Minerals, Metals and Materials Society: Warrendale, PA, 1996; p 457.
(20) Üstündag, E.; Subramanian, R.; Dieckmann, R.; Sass, S. L. *In Situ Comps. Proc. Symposium*; Singh, M., Lewis, D., Eds.; Met. Mater. Soc.: Warrendale, PA, 1994; p 97.
(21) Huggins, R. A.; Nix, W. D. *Ionics* **2000**, *6*, 57.
(22) Wang, J.; Raistrich, I. D.; Huggins, R. A. *J. Electrochem. Soc.* **1986**, *133*, 457.

Li_3Sb, as illustrated in Figure 1. We compare the starting oxides $SbVO_4$ and $Sb_2Mn_2O_7$ because they have different crystal structures and transport characteristics. Sb takes on 5+ valence in both compounds, while V and Mn have 3+ and 2+ valence, respectively.[23,24] The standard free energy of formation for Sb_2O_5 ((−330 kJ/mol)/O_2) is much less negative than that for V_2O_3 ((−757 kJ/mol)/O_2) or MnO ((−723 kJ/mol)/O_2).[25] [While the standard free energy of oxidation for each of the component oxides (Sb_2O_5, V_2O_3, MnO) will in principle differ in the mixed oxides from the values for the pure oxides, we sucessfully carried out partial reduction using data for the pure oxides as guidance.] Consequently, conditions of temperature and oxygen activity are easily chosen which thermodynamically favor the partial reduction of Sb oxide to its metal from either of the mixed compounds. $SbVO_4$ has the rutile structure in which lattice cation diffusion of both species is expected to be more rapid than oxygen diffusion; hence, the kinetics of partial reduction analyzed by Schmalzried et al.[11] apply. Due to the high Sb fraction, external reduction may occur in this system. $Sb_2Mn_2O_7$, in contrast, has a fluorite derivative structure[26] in which oxygen diffusion is much more rapid than cation diffusion. In this case, internal reduction is expected. The rates of partial reduction were not known a priori for either system, but experiments showed that complete reduction of the antimony oxide to its metal is readily accomplished at low temperatures (<400 °C) in a few hours in a flowing stream of commonly available inert or reducing gases.

Experimental Section

$SbVO_4$ and $Sb_2Mn_2O_7$ were prepared using the solid-state reaction of Sb_2O_3, V_2O_3, and $MnCO_3$. The reacted powders were deagglomerated by Spex-milling using a zirconia jar. In each instance, XRD was used to confirm the presence of predominantly a single-phase compound prior to partial reduction. For partial reduction, a small amount (0.4−2 g) of each powder was heated in an alumina boat (with powder depth ∼ 2 mm) in a tube furnace at temperatures and oxygen activities that thermodynamically favored the reduction of the first metal. Both buffered CO/CO_2 gas mixtures and unbuffered pure H_2 gas at 1 atm total pressure were used. In the case of CO/CO_2, the temperature and oxygen activity can be selected to reduce only the antimony oxide. In the case of hydrogen gas, equilibrium would eventually favor reduction of all the oxides to their metals. Nonetheless, it was possible to choose conditions that reduce the antimony while retaining a single phase of the transition metal oxide. X-ray diffraction (Rigaku RU300, Cu Kα radiation) and weight loss were used to determine the phases present and the extent of reduction. JEOL 2000FX and 2010FX transmission electron microscopes (TEM), a Fisons HB603 scanning transmission electron microscope (STEM), and a Philips XL30 environmental scanning electron microscope (ESEM) were used to characterize the sample microstructures and phases.

Electrodes consisting of 70−88 wt % of the sample, 5−10 wt % carbon additive, and 10−20 wt % of poly(vinylidene fluoride) binder (Aldrich) were prepared. These were mixed with γ-butyrolactone solvent (98%, Alfa Aesar) and either cast onto a sheet of Cu foil or dried and then pressed at 4000 kg/cm^3 into $^1/_4$ in. diameter pellets. All electrodes were tested in stainless steel cells using Li foil (Alfa Aesar) as the reference electrode, EC:DMC (1:1 by weight) with 1 M $LiPF_6$ (EM Science) as the electrolyte, and Cellgard 2400 as the separator. Cycling was conducted at room temperature at current densities and voltage ranges given later. Certain of the carbon additives (Ensaco 350 or Super P, Chemetals Inc.) made a significant contribution to both the first-cycle irreversible capacity loss and reversible capacity of the electrodes. When the samples were formulated into electrodes and tested separately, up to 545 mAh/g of carbon and up to 80 mAh/g irreversible capacity was seen on the 1st discharge in the 0.7−1.3 V range. The capacity data corrected by subtracting the capacity contribution of the added carbon from the total electrode capacity.

Results and Discussion

Materials Characterization. Partial reduction was successfully completed at 400 °C (4 h, H_2, 140 SCCM flow rate) for $SbVO_4$ and 360 °C (18 h, H_2, 140 SCCM flow rate) for $Sb_2Mn_2O_7$. Figure 2 shows XRD patterns of the starting oxides and their partially reduced counterparts, respectively. In the case of $SbVO_4$, the oxide phase coexisting with Sb metal after partial reduction was determined by XRD to be V_2O_3. In the case of $Sb_2Mn_2O_7$, XRD showed the remaining oxide to be MnO. In both cases, the oxide peaks were broad, indicating disorder or ultrafine grain size. Multiple SEM and TEM observations on the microstructures of the samples were made. SEM images showed that there was a dramatic difference in the Sb precipitate size between the two types of samples (Figure 3). Partially reduced $SbVO_4$ contained external Sb metal precipitates of octahedral morphology as large as 20 μm in size, mixed with V_2O_3 particles. The partially reduced $Sb_2Mn_2O_7$ exhibited much finer Sb surface precipitates of ∼2 μm size by SEM. In this material, TEM also revealed dispersed Sb precipitates of ∼20 nm size within the oxide matrix, as seen in Figures 4 and 5. Electron diffraction showed that the oxide matrix was either nanocrystalline MnO (Figure 4) or amorphous manganese oxide (Figure 5), both coexisting in the same sample. On the basis of the weight loss upon partial reduction, the disordered phase also appears to be MnO. Thus the partial reduction reactions for these two systems are

$$SbVO_4 \rightleftharpoons Sb\ (metal) + 1/2V_2O_3 + 5/4O_2(g) \quad (2)$$

$$Sb_2Mn_2O_7 \rightleftharpoons 2\ Sb(metal) + 2MnO + 5/2O_2(g) \quad (3)$$

The disorder occurring in the remaining transition metal oxide can be understood from the fact that a reconstructive transformation is required. For example, in the fluorite, the oxygen sublattice is not close-packed and Mn occupies 8-fold coordinated sites, whereas, in the rocksalt structure-type MnO product, oxygen is close-packed and Mn is 6-fold coordinated. It is evident that the temperatures and times used for partial reduction are not sufficient for complete crystallization of product oxides. Thus partial reduction in these instances may also be considered a solid-state amorphization process. Solid-state amorphization occurs when a metastable amorphous phase forms instead of the thermo-

(23) Brisse, F.; Stewert, D. J.; Seide, V.; Knop, O. *Can. J. Chem.* **1972**, *50*, 3648.
(24) Salmon, R.; Graciet, M.; Le Flem, G. *C. R. Acad. Sci.* **1976**, *282*, 795.
(25) *CRC Handbook of Chemistry and Physics*; Lide, D. R., Ed.; CRC Press: Boston, MA, 1990.
(26) Scott, H. G. *J. Solid State Chem.* **1987**, *66*, 171.

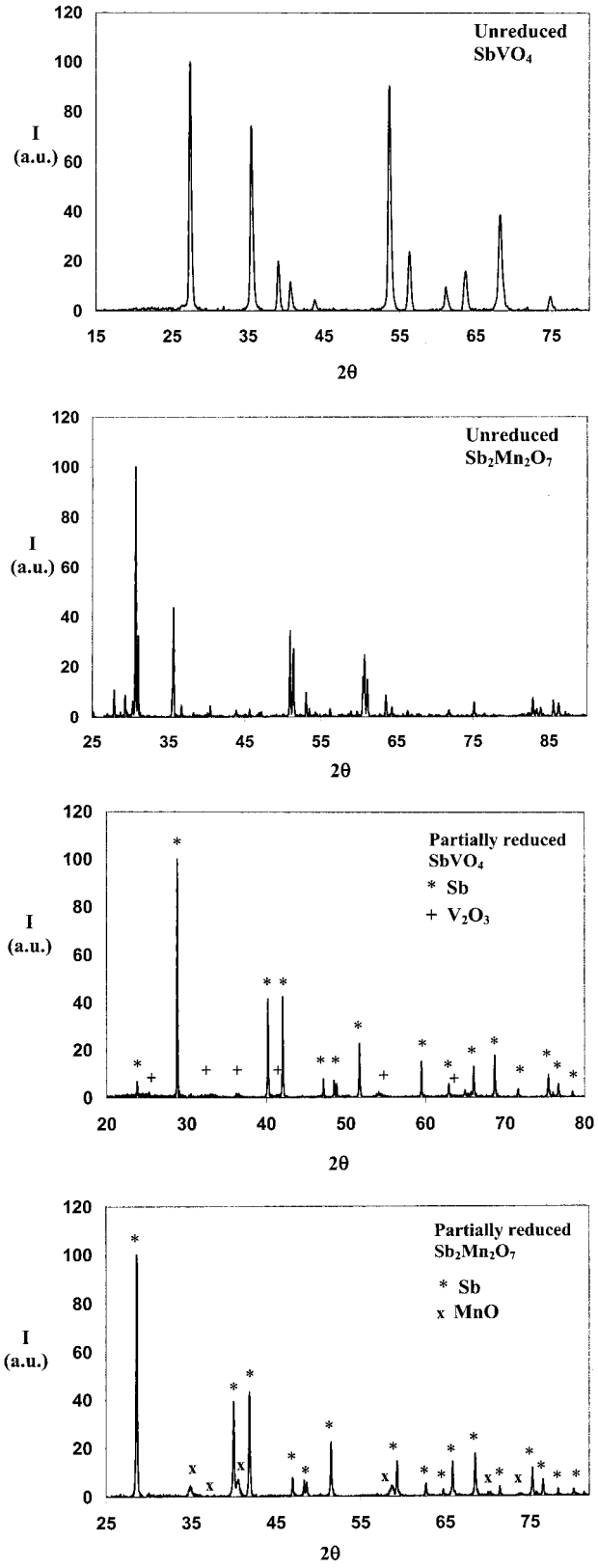

Figure 2. X-ray diffraction patterns of the starting oxides $SbVO_4$ and $Sb_2Mn_2O_7$ and their partially reduced counterparts.

dynamically preferred crystalline phase due to kinetic limitations. It has previously been observed in multilayer thin films[27] and at surfaces and interfaces.[28,29]

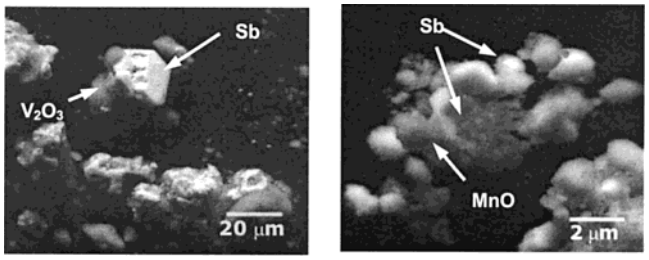

Figure 3. SEM images of partially reduced $SbVO_4$ and $Sb_2Mn_2O_7$ powders. Note the much larger Sb metal precipitate size in the former material, which is attributed to external reduction followed by coarsening.

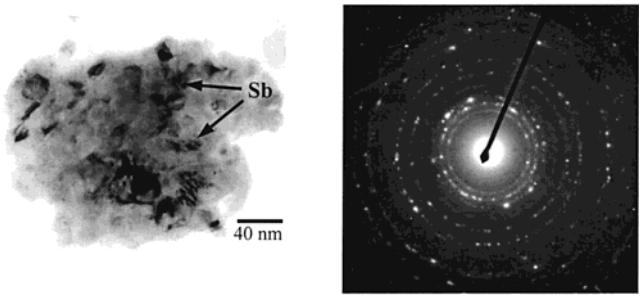

Figure 4. Sb−MnO nanocomposite particle formed by the partial reduction of $Sb_2Mn_2O_7$. The electron diffraction pattern shows the presence of crystalline Sb metal and MnO.

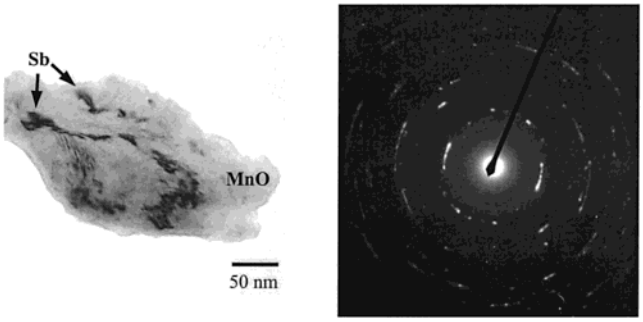

Figure 5. Sb−MnO nanocomposite particle in which dispersed nanocrystalline Sb metal forms within a matrix of amorphous MnO.

Amorphization upon partial reduction has not previously been reported but may be useful as a process for creating chemically and electrochemically active solids.

We expected the internal reduction observed in the $Sb_2Mn_2O_7$, on the basis of the high oxygen diffusivity relative to cation diffusivity. Even in such instances, however, some metal precipitates can nucleate and grow at the surface of the oxide particle. The fraction of external precipitates is limited by the Sb diffusion length during the heat treatment, although they may coarsen rapidly once formed due to the high vapor pressure of Sb.[25] This explains the simultaneous formation of external and internal precipitates in the case of the $Sb_2Mn_2O_7$ (Figure 3). It is expected that as the $Sb_2Mn_2O_7$ particle size increases, the fraction of the total Sb that is internally precipitated will also increase.

Electrochemical Properties. The Sb−V_2O_3 and Sb−MnO composites showed similar first-cycle voltage profiles (Figure 6), with an average voltage plateau

(27) Johnson, W. L. *Materials Interfaces*; Wolf, D., Yip, S., Eds.; Chapman and Hall: New York, 1992; p 517.

(28) Wang, H.; Chiang, Y.-M. *J. Am. Ceram. Soc.* **1998**, *81* (1), 89.
(29) Luo, J.; Chiang, Y.-M. *Acta Mater.* **2000**, *48*, 4501.

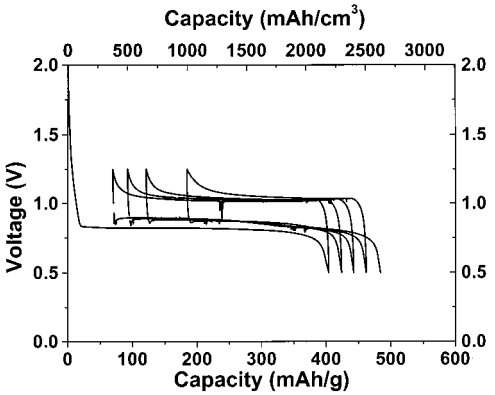

Figure 6. Voltage−capacity curves for the first few cycles of an Sb−V_2O_3 composite (20 mA/g), showing an average voltage plateau near 0.97 V as expected for the alloying of Li with Sb. Similar results were observed for Sb−MnO samples.

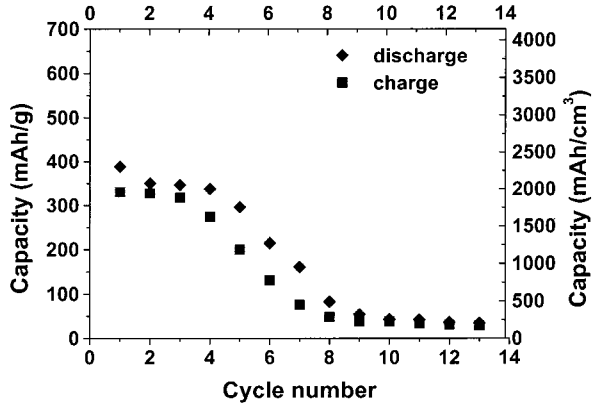

Figure 7. Capacity vs cycle number ($V = 0.5-1.25$ V, 20 mA/g) for Sb−V_2O_3 samples with large external precipitates of Sb metal. Note the rapid capacity fade in the first few cycles.

between charge and discharge plateaus of ∼0.97 V, corresponding to Li alloying with Sb metal.[22] Closer examination revealed two closely spaced plateaus upon discharge, corresponding to the formation of Li_2Sb and Li_3Sb, respectively.[22] Upon deeper discharge, our experiments reveal a reversible displacement reaction of MnO, occurring at plateau voltages of ∼0.4 and 0.25 V. This is similar to the displacement reactions used in primary batteries,[30] which is usually poorly reversible and which Tarascon et al. have recently reported can be more reversible in the case of CoO.[31] To observe the alloying with Sb, we chose the lower voltage cutoffs to be 0.5−0.7 V, above that for the displacement reaction.

It was observed that there are significant differences in capacity retention between the $SbVO_4$-derived coarse Sb precipitates and the $Sb_2Mn_2O_7$-derived nanocomposite. As shown in Figures 7 and 8, rapid capacity fade in the first several cycles was observed for the former, while the latter exhibited much better capacity retention to ∼20 cycles. With further cycling, most of the Sb−MnO cells showed sudden capacity fade at the 20th to 25th cycle (Figure 8). However, this characteristic was found to be related to cell failure rather than materials failure. Upon disassembling a faded cell and reassembling using a new lithium electrode, separator, and

(30) Vincent, C. A.; Scrosati, B. *Modern Batteries*; John Wiley & Son: London, 1997; p 124.

(31) Poizot, P.; Laruelle, S.; Grugeon, S.; Dupont, L.; Tarascon, J. M. *Nature* **2000**, *407*, 496.

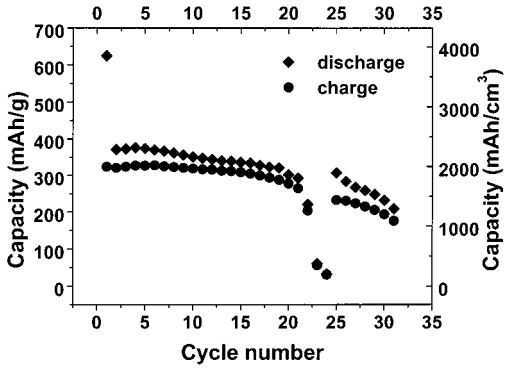

Figure 8. Capacity vs cycle number ($V = 0.7-1.3$ V, 14 mA/g) for Sb−MnO samples containing fine external precipitates (Figure 3) and nanocrystalline internal precipitates of Sb metal. After 24 cycles, the cell was disassembled and the lithium electrode, electrolyte, and separator were replaced.

electrolyte, we found that the capacity was mostly restored (Figure 8), the difference being attributable to some loss (∼10%) of the active material from the electrode during handling and reassembly of the cell. All cycled cells showed a rough solid−electrolyte interface (SEI) on the lithium metal electrode, even after only a few cycles. The Coulombic inefficiency seen in the cycling data (Figures 6−8) may correspond to a side reaction that forms the SEI. Further experimentation is, therefore, necessary to find a cell chemistry that allows the true long-term cycling behavior of these materials to be determined. However, even within the present testing limitations, the results in Figure 8 show that capacity retention is excellent to a minimum of 20 cycles. This is remarkable reversibility for a system in which the active compound (Sb) expands by a factor of 2.36 upon alloying, and can be directly attributed to the nanocomposite morphology.

Upon lithiation of Sb to Li_3Sb, the theoretical capacities of Sb + V_2O_3 and Sb + MnO composites produced from $SbVO_4$ and $Sb_2Mn_2O_7$ are 408.9 mAh/g (2423 mAh/cm^3) and 417.3 mAh/g (2575 mAh/cm^3), respectively. The initial charge (delithiation) capacities in Figures 7 and 8 are close to these values, supporting the nearly complete reduction of the Sb oxide to active metal during the thermochemical reduction process. The volumetric capacities of the composites are particularly attractive in comparison to those for carbon anodes (837 mAh/cm^3). For the Sb−MnO sample in Figure 8, the first discharge capacity exceeds the theoretical value, indicating lithium uptake elsewhere in the material upon first insertion, possibly in the disordered MnO. We believe that control of crystallinity and morphology of both phases in the composite will lead to further improvements in the electrochemical properties.

Conclusions

The thermochemical partial reduction of mixed oxides has been demonstrated as a new approach to synthesizing metal−ceramic nanocomposites for lithium storage. Selection criteria are presented for choosing mixed oxide compounds which can be selectively reduced to form electrochemically active metal−ceramic composites. Results show that the partial reduction approach can be used to create electrochemically active metal−ceramic composites with a variety of microstructures and that

the electrochemical properties are directly coupled to the microstructures that are obtained. A comparison of two Sb-containing oxides, $SbVO_4$ and $Sb_2Mn_2O_7$, shows that greatly improved resistance to cycling fade is obtained for the latter, in which a nanoscale internal dispersion of the lithium-active metal in the oxide matrix is obtained. Through this approach, high gravimetric and volumetric capacities are possible while using inexpensive starting materials and relatively simple, scalable, thermochemical processes.

Acknowledgment. Funding and instrumentation in the Shared Experimental Facilities at MIT were supported by NSF Grant No. 9400334-DMR.

CM0014280